Impact of Pellet Injection on Extension of Operational Region in LHD

R. Sakamoto [1)], H. Yamada [1)], K. Tanaka [1)], K. Narihara [1)], S. Morita [1)], S. Sakakibara [1)], S. Masuzaki [1)], L.R. Baylor [2)], P.W. Fisher [2)], S.K. Combs [2)], M.J. Gouge [2)], S. Kato [1)], A. Komori [1)], O. Kaneko [1)], N. Ashikawa [3)], P. de Varies [1)], M. Emoto [1)], H. Funaba [1)], M. Goto [1)], K. Ida [1)], H. Idei [1)], K. Ikeda [1)], S. Inagaki [1)], M. Isobe [1)], S. Kado [1)], K. Kawahata [1)], K. Khlopenkov [1)], S. Kubo [1)], R. Kumazawa [1)], T. Minami [1)], J. Miyazawa [1)], T. Morisaki [1)], S. Murakami [1)], S. Muto [1)], T. Mutoh [1)], Y. Nagayama [1)], Y. Nakamura [1)], H. Nakanishi [1)], K. Nishimura [1)], N. Noda [1)], T. Notake [4)], T. Kobuchi [3)], Y. Liang [3)], S. Ohdachi [1)], N. Ohyabu [1)], Y. Oka [1)], M. Osakabe [1)], T. Ozaki [1)], R.O. Pavlichenko [1)], B.J. Peterson [1)], A. Sagara [1)], K. Saito [4)], H. Sasao [3)], M. Sasao [1)], K. Sato [1)], M. Sato [1)], T. Seki [1)], T. Shimozuma [1)], M. Shoji [1)], S. Sudo [1)], H. Suzuki [1)], M. Takechi [1)], Y. Takeiri [1)], N. Tamura [3)], K. Toi [1)], T. Tokuzawa [1)], Y. Torii [4)], K. Tsumori [1)], I. Yamada [1)], S. Yamaguchi [1)], S. Yamamoto [4)], Y. Yoshimura [1)], K.Y. Watanabe [1)], T. Watari [1)], K. Yamazaki [1)], Y. Hamada [1)], O. Motojima [1)] and M. Fujiwara [1)]

1) National Institute for Fusion Science, Toki, Japan
2) Oak Ridge National Laboratory, Oak Ridge, TN, USA
3) Department of Fusion Science, Graduate University for Advanced Studies, Hayama, Japan
4) Department of Energy Engineering and Science, Nagoya University, Nagoya, Japan

E-mail: sakamoto@LHD.nifs.ac.jp

Abstract: Pellet injection has been used as a primary fueling scheme in Large Helical Device (LHD). Pellet injection has extended an operational region of NBI plasmas to higher densities with maintaining preferable dependence of energy confinement on density, and achieved several important data, such as plasma stored energy (0.88 MJ), energy confinement time (0.3 s), β (2.4 % at 1.3 T) and density (1.1×10^{20} m^{-3}). These parameters cannot be attained by gas puffing.

Ablation and subsequent behavior of plasma has been investigated. Measured pellet penetration depth that is estimated by duration of the Hα emission is shallower than predicted penetration depth from the simple neutral gas shielding (NGS) model. The penetration depth can be explained by NGS model with fast ion effect on the ablation. Just after ablation, redistribution of ablated pellet mass was observed in short time (~ 400 μs). The redistribution causes shallow deposition and low fueling efficiency.

1. Introduction

Through the study of inter-machine scalings of energy confinement time [1,2], confinement in currentless helical plasmas has been proved to be comparable to in tokamaks while preferable dependence on electron density is more pronounced than in tokamaks. The international stellarator scaling 95 (ISS95) is described as follows.

$$t_E^{ISS95} = 0.079\, a_p^{2.21} R_0^{0.65} P_{abs}^{-0.59} \bar{n}_e^{0.51} B_0^{0.83} \dot{\iota}_{2/3}^{0.40}.$$

Gas puffing has been successful for building up and sustaining the plasma density in the past generation fusion plasma experiments. However, inevitability of gas puffing is questionable in large-scale, high-temperature and steady state fusion plasmas since the plasma sources are strongly localized at the plasma surface. Especially gas puffing is not efficient in LHD, because the core plasma region is surrounded with the thick ergodic layer that connects to the divertor. Efficient fueling to the core plasma would be mandatory in large plasmas. Hydrogen ice pellet injection is one of the important techniques used for core plasma fueling. In the LHD experiment, pellet injector is placed as a fundamental tool since deterioration of fueling efficiency by gas puffing is a concern.

The ablation mechanism and the subsequent density redistribution affect fueling efficiency and fueling depth [3,4]. Since a dramatic increase in pellet velocity, which can enhance deep fueling, poses a difficult problem in technology, optimization based on physical understanding of the mechanism of these processes is required.

The main aim of the present study is to reveal pellet ablation behavior and effect of pellet injection on plasma, and to examine the validity of the pellet fueling in LHD.

2. Experimental set-up

Experiments were carried out on Large Helical Device (LHD), a heliotron type magnetic confinement device with super conducting coils [5,6]. The major radius, averaged minor radius, magnetic field and plasma volume are 3.9 m, 0.6 m, 2.9 T and 30 m^3, respectively.

The pellet injector used on LHD is a pneumatic pipe-gun type accelerator with a GM cycle refrigerator [7]. The injector is equipped with five barrels and can inject independently any desired time. The mass and velocity of pellets are $0.4 – 1.0\times10^{21}$ atoms per pellet and 900 – 1200 m/s, respectively. Cylindrical pellets formed from high purity hydrogen gas were injected horizontally from the outer side mid-plane of LHD. Pellet mass was measured by a microwave cavity mass detector, and velocity was measured by the time of fright method. The injected pellets were check by a shadow graph system, which consists of a fast flash lamp and a CCD camera at the exit of the injector.

Pellet injection experiment has been carried out mainly for NBI heated plasmas. LHD is equipped with two negative-ion based neutral beam injectors. The range of beam energy and port through power is 120 – 150 keV and 1 – 4.5 MW, respectively.

Pellet ablation was measured by a fast photo diode (500 kHz sampling) and a CCD camera (each 33 ms exposure) with a Hα (656.5 nm) filter. A variety diagnostics were used to investigate the plasma behavior after pellet injection. For instance, line-averaged electron densities $\bar{n}_e$ were measured by a 13-chord vertical view far-infrared (FIR) laser interferometer [8], which was installed at the distance 168° in the toroidal angle from the pellet injection port. Profiles of electron temperature T_e and electron density n_e were measured by the multi-point (200) Thomson scattering system [9], which was installed at the distance 30° in toroidal angle. Electron density profile based on Thomson scattering was calibrated by Abel inverted FIR interferometer data just before pellet injection.

3. Extension of operational region following pellet injections

Waveforms for typical pellet injected discharge are shown in figure 1 Pellet injection was carried out at 0.8,0.88, 0.96, 1.04 and 1.12 s. The line averaged electron

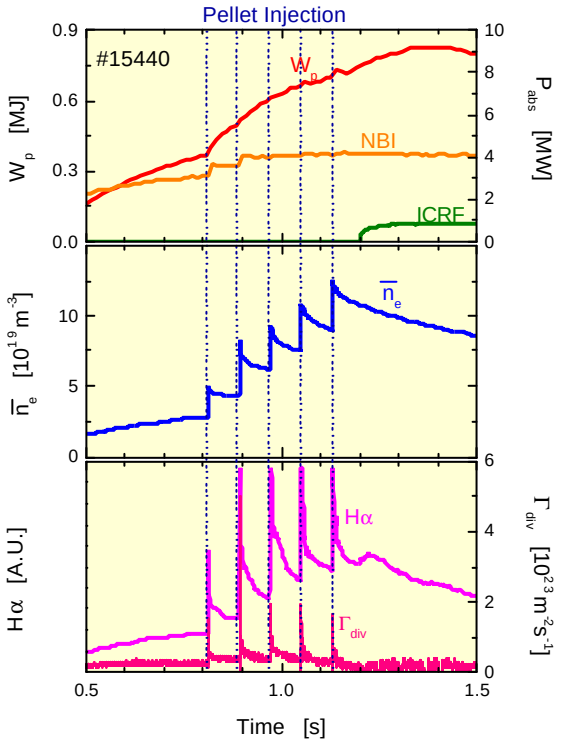

Figure 1. Waveform of typical pellet injected discharge. (#15440, B_t= 2.75 T, R_{ax}= 3.6 m, P_{NBI}= 4 MW).

density increases sharply at each pellet injection and a burst in the Hα intensity and divertor flux is observed simultaneously. Figure 2 shows plots of the normalized maximum stored energy versus the density when the stored energy achieved to maximum. Predicted dependence by the international stellarator scaling 95 (ISS95) is shown with dashed lines. Since systematic enhancement in energy-confinement time from the scaling has been observed in LHD [10], 1.7 times of the prediction is also shown. In the case of gas puffing, confinement degradation was observed at density above 0.35×10^{20} m^{-3} and the maximum density is 0.5×10^{20} m^{-3}. On the other hand, in the pellet injection discharges no obvious density-related confinement degradation has been observed beyond predicted the density limit, and the stored energy reaches to 0.88 MJ.

Figure 3 shows maximum line averaged electron density versus NBI power. Solid line indicate the predicted density limit in the stellarator/heliotron device. The density limit can be expressed as follows [2],

$$n_c^s = 0.25\sqrt{P B / a^2 R}\,.$$

where P, B, a and R are the heating power, the magnetic field strength, the minor radius and the major radius, respectively. In the case of gas puffing, an envelope of the data conforms well to the predicted density limit. In the case of pellet injection, the maximum density reaches to high density beyond predicted density limit.

4. Ablation behaviors and density redistribution

Neutral gas shielding (NGS) model [11][12], which is the most widely adopted ablation model. If one assumes pellet injection normal to the plasma from the outside midplane and linear profiles for electron temperature and density, the penetration depth scaling of the NGS models is expressed as follows [13],

$$\lambda/a = C\, T_e^{-5/9}\, n_e^{-1/9}\, m_p^{5/27}\, v_p^{1/3},$$

where T_e, n_e, m_p and V_p are the central electron temperature, the central electron density, the pellet mass and the pellet velocity, respectively. The scaling suggests that the penetration depth

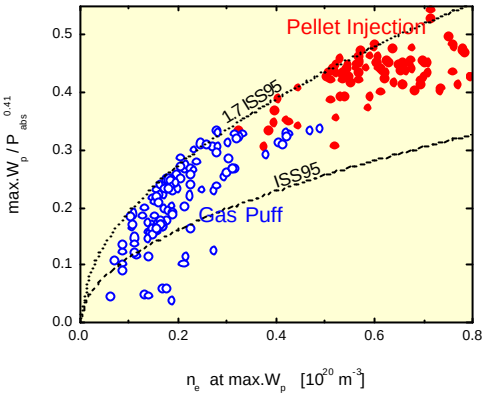

Figure 2. Normalized maximum plasma stored energy versus line averaged electron density. Open circle and close circle indicate data of gas puffing and pellet injection, respectively. Dashed line showISS95 scaling prediction.

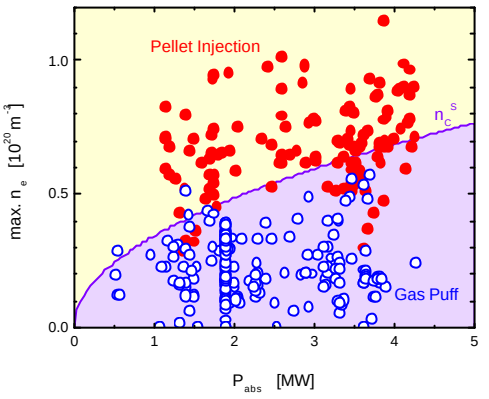

Figure 3. Maximum line averaged electron density versus NBI power. Open circle and close circle indicate data of gas puffing and pellet injection, respectively. predicted density limit is show with solid line.

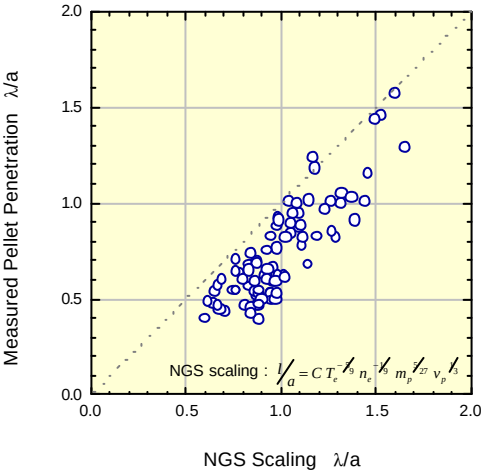

Figure 4. Comparison of the measured penetration depth versus the scaling.

depends mainly on the electron temperature. Measured penetration depth is compared with the NGS scaling in Figure 4. Measured penetration depth of the pellet is estimated by duration of Hα emission from ablating pellet on the assumption that velocity of the pellet is constant during ablation. The trend of the measured penetration depth agrees approximately with NGS scaling, but the measured penetration depth is systematically shallower than NGS scaling. This systematical difference can be explained by effect of fast ions on the ablation. There is no Ohmic heating in LHD and the NBI is only heating source. Figure 5 shows the profiles before and after pellet injection into 3.1 MW NBI heated plasma. (a) shows the density and calculated beam component density [14]. (b) shows the electron temperature,. Since beam component density is comparable to electron density in such a low density plasma, effect of fast ions on the ablation can not be ignored. Figure 5 (c) shows deposition profiles that are calculated from the NGS model using ABLATE code [15] which can take effect of fast ions on the ablation, and the Hα emission from ablating pellet mapped onto the normalized minor radius is also shown. Calculated deposited density profile with fast ion ablation indicates a good agreement with Hα emission measurement. On the other hand, measured deposition peak is shifted outward as compared with Hα emission peak, and majority of pellet mass was deposited outside of $r = 0.8$. As a result, a net fueling efficiency is 46 %. This profile shift suggest redistribution of pellet mass on the fast time scale. Similar phenomena has been observed in DIII-D [4]. Figure 6 shows high time resolution waveform at the timing of pellet ablation. Line averaged electron density is divided into two part, core density $\bar{n}_e^{core}$ (r<0.7) and boundary density $\bar{n}_e^{boundary}$ (r>0.7), using multi-chord interferometer data. Ablation starts at 0.511 s. About the same time boundary density starts to increase, then core density start to increase. Core density increase is stopped and then starts to decrease at the same time the ablation is finished (0.5114 s). Contrary to this, boundary density increases further. The core

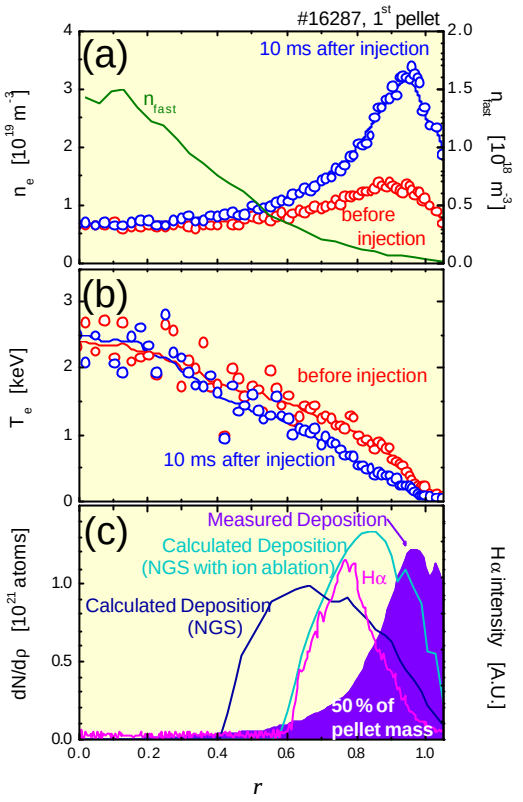

Figure 5. Radial profiles before and after pellet injection. (a) electron density and calculated beam component density, (b) electron temperature, (c) Ha intensity which indicates pellet penetration depth, measured deposition and calculated deposition.

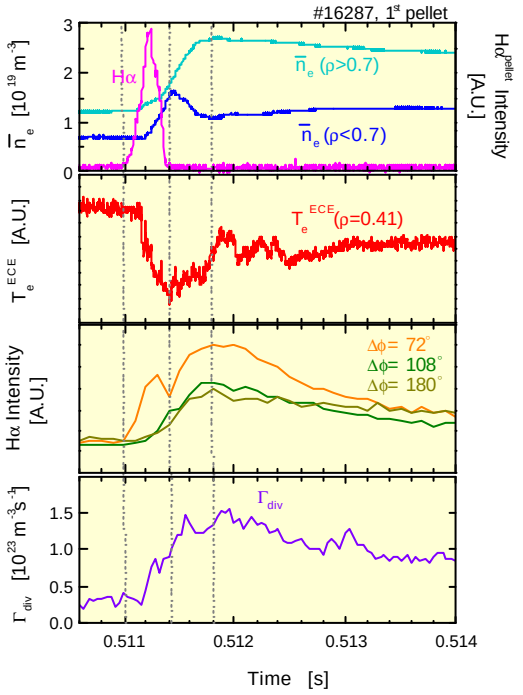

Figure 6. Temporal evolution of pellet injected plasma at the timing of ablation.

density decrease and boundary density increase stop at 0.5118 s (400 μs after ablation). These phenomena can be explained as follows: Though pellet penetrates into a certain depth that is well predicted by the NGS with fast ion ablation, a noticeable part of pellet mass are spewed out from the core region, pellet mass redistribute in a short time (~ 400 μs). On the other hand, electron temperature at ρ=0.41 indicate the inverse behavior to core density evolution, therefore pellet mass redistribute adiabatically. Hα emission except for ablating pellet grows in the core density decay phase which is distinct in the apart toroidal position, and divertor flux also increase at the same time.

5. Summary and future plan

Pellet injection has extended an operational region of NBI plasmas to higher densities with maintaining preferable dependence of the energy confinement on the density beyond the gas-fueling conditions. At the current stage of experiment, attained density was restricted by the supply mass of the pellet and/or the lack of heating power. A hard density limit has not been observed in LHD yet, it is a important issue to investigate on the confinement property and density limit in the further high density regime in helical systems.

Though penetration depth of the pellet is explained qualitatively by a simple NGS model, When fast ion effect on the ablation is considered in NGS model, a quantitative agreement between measurement and calculation has been obtained. However, expulsion of the pellet mass was observed on the fast time scale (~several 100 μs) just after ablation, which causes degradation of fueling efficiency. Because a same phenomenon is observed in tokamak, it is consider that there is a general physical mechanics on density redistribution. Improvement of the pellet fueling by means of the magnetic high field side injection has been reported in tokamak [3][4]. We have plan of inner port injection in the coming LHD experimental campaign which start at the beginning of October, 2000. The mechanism on density redistribution will be revealed through comparative study in different magnetic configurations.

The authors are grateful to the device-engineering group for their operational support.

Reference

[1] Stroth, U., et al., Nuclear Fusion, 36 (1996) 1063-1077.
[2] Sudo, s., et al., Nuclear Fusion, 30 (1990) 11-21.
[3] Lang, P.T., et al., Physical Review Letters, 79 (1997) 1487-1490.
[4] Baylor, L.R., et al., Fusion Technology, 34 (1998) 425-429.
[5] Fujiwara, M., et al., Journal of Fusion Energy, 15 (1996) 7-153.
[6] Motojima, O., et al., Physics of Plasmas, 6 (1999) 1843-1850.
[7] Yamada, H., et al., to be published on Fusion Engineering and Design.
[8] Kawahata, K., et al., Fusion Engineering and Design, 34-35 (1997) 393-397.
[9] Narihara, K., et al., Fusion Engineering and Design, 34-35 (1997) 67-72.
[10] Yamada, H., et al., Physical Review Letter, 84 (2000) 1216-1219.
[11] Parks, P.B., et al., Nuclear Fusion, 17 (1977) 539-556.
[12] Milora, S.L., et al., IEEE Transaction on Plasma Science, PS-6 (1978) 578-592.
[13] Baylor, L.R., et al., Nuclear Fusion, 37 (1997) 445-450.
[14] Murakami, S., et al., Fusion Technology, 27 (1995) 256-259.
[15] Nakamura, N., et al., Nuclear Fusion, 26 (1986) 907-921.